

Molecular adsorption on the (0001) surfaces of rare-earth metalsR. I. R. Blyth,^{1,2,*} C. Searle,² N. Tucker,² R. G. White,² T. K. Johal,^{1,2} J. Thompson,¹ and S. D. Barrett²¹*National Nanotechnology Laboratory of INFN, Dipartimento di Ingegneria dell'Innovazione, Università di Lecce, Via Arnesano, 73100 Lecce, Italy*²*Surface Science Research Centre and Department of Physics, University of Liverpool, Liverpool L69 3BX, United Kingdom*

(Received 21 March 2003; revised manuscript received 1 August 2003; published 5 November 2003)

The adsorption of molecules on rare-earth (0001) thin films on W(110) at room temperature has been studied using photoemission spectroscopy. CO₂ adsorbs dissociatively, up to monolayer coverage, forming a carbonate species, with clean up of adventitious hydrogen also observed. Higher coverages result in molecular adsorption. H₂O and H₂S on Y(0001) also adsorb dissociatively, resulting in atomic H and S, up to monolayer coverage. Higher coverages of H₂O result in oxidation of the substrate to Y₂O₃, with formation of H₂O multilayers. H₂S dissociation appears to result in atomic S, adsorbed in both hollow and bridge sites. No indication of CH₄ adsorption was seen on Y(0001). These results, and those from the literature, are compared to data from bulk single-crystal rare-earth (0001) surfaces in an attempt to explain the origin of certain unexplained photoemission features observed on those surfaces.

DOI: 10.1103/PhysRevB.68.205404

PACS number(s): 79.60.Dp, 73.20.Hb, 71.20.Eh

I. INTRODUCTION

Although the preparation of clean, well-ordered (0001) surfaces of the rare-earth metals, in the form of thin films grown *in situ* on W(110), has been known for almost 20 years,¹ the number of studies of adsorbates on these surfaces remains small. Given that the rare earths and their compounds exhibit catalytic activity, the motivation for a large percentage of surface science investigations of molecules on other metal surfaces, this is rather surprising. In addition, there has been some recent interest in using rare-earth metals as contact materials in devices based on organic molecules,^{2,3} so the interaction of molecules with rare-earth surfaces is not without interest. Despite this, the literature contains only studies of the relatively simple diatomic molecules hydrogen,⁴⁻⁷ oxygen,^{6,8-12} nitrogen,¹³ and carbon monoxide^{6,14} on well-characterized rare-earth metal (0001) films. All these studies have indicated dissociative adsorption of the molecules studied. In this work we extend the range of photoemission studies of adsorbates on rare-earth metal (0001) surfaces to the larger molecules CO₂, H₂O, H₂S, and CH₄.

Gd(0001) is the most widely studied rare-earth metal surface, due largely to its magnetic properties, and all the published rare-earth (0001) adsorbate studies have been of this surface. However, Gd is not particularly suited to photoemission studies of adsorbates as the prominent *4f* peak, at ~8 eV binding energy,¹⁵ falls well within the spectroscopic region where molecular orbitals would be expected to be observed. For a direct comparison with the results for CO (Refs. 6,14) we used Gd(0001) as the substrate for the CO₂ experiments, but for the other molecules we used Y(0001). Although yttrium is very much lighter, it is often grouped, from the point of view of chemical behavior, with the heavy lanthanides (i.e., Gd-Lu). Indeed, bandstructure calculations¹⁶ show that its electronic structure is very similar to that of Gd.¹⁷ It is therefore well suited as a prototypical rare earth for photoemission studies, since obviously it has no *4f* electrons to complicate the spectra. For the true heavy

lanthanides, the *4fs* are significant features in the binding-energy range 0–12 eV,¹⁵ clearly intruding upon the spectral range of molecular adsorbates. Although the *4fs* lie close to the valence band, they are highly localized spatially, and while being responsible for the magnetic behavior, play little or no role in chemical bonding. Y and Gd have a further chemical similarity, in that they both have a stable trivalent configuration, ensuring that they cannot exhibit the redox reactions typical of cerium-based catalysts.¹⁸⁻²⁰ This is not true of, among the heavy lanthanides, Tb, Tm, and especially Yb, whose mixed-valence behavior is well known.

The addition of these data to those already published allows a comparison of the spectra of single-crystal rare-earth metal (0001) surfaces with those of thin film (0001) surfaces “contaminated” by a wide range of species, in an attempt to understand the origin of unexplained features on the nominally clean single-crystal surfaces.

II. EXPERIMENT

The experiments were performed on beamline 4.1 (Ref. 21) at the Synchrotron Radiation Source, Daresbury Laboratory, UK, using a Vacuum Science Workshop HA54 angle-resolved analyzer in a vacuum chamber with a base pressure <10⁻¹⁰ mbar. All spectra were recorded at normal emission, using *p*-polarized light, incident at 30°. For valence-band photoemission spectra, a photon energy of 40 eV was used, with an overall energy resolution (beamline plus analyzer) of 0.15 eV. For Y *4p* and S *2p* spectra, photon energies of 60 eV (resolution 0.3 eV) and 195 eV (resolution 0.8 eV) were used, respectively. Thin films of Y(0001) and Gd(0001) were prepared on W(110) as described in Ref. 22. CO₂, H₂S, and CH₄ (99.997% pure) were obtained from Gas Distillers, while distilled water was further purified by a series of freeze-thaw cycles. The molecules were dosed by background exposure, with the purity checked by mass spectrometer, and the quoted dosages derived from uncorrected ion gauge readings. Due to technical difficulties, a full dosing series for H₂S on Y(0001) was not possible. All

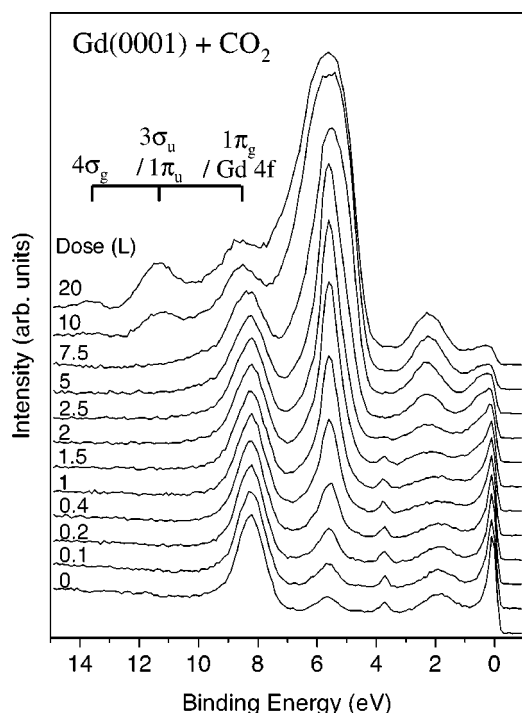


FIG. 1. Photoemission spectra ($h\nu=40$ eV) of Gd(0001) with increasing exposure to CO_2 . The assignments for the molecular orbitals of CO_2 are also shown.

dosing and photoemission measurements were performed at room temperature.

III. RESULTS

A. CO_2 on Gd(0001)

Photoemission spectra of increasing doses of CO_2 on Gd(0001) are shown in Fig. 1. The as-prepared surface shows the intense surface state close to the Fermi level characteristic of relatively clean, well-ordered rare-earth (0001) metal surfaces.^{23,24} Note that since the surface state persists even with significant contamination levels, the mere presence of the surface state cannot be taken as indicating a contamination-free surface, as the literature sometimes implies. The peak at 2 eV binding energy is due to Δ_2 bulk bands,²⁵ with the 4*f* peak appearing at 8.3 eV.¹⁵ There are also peaks at ~ 6 eV and ~ 4 eV due to adventitious oxygen⁹ and hydrogen,⁴ respectively. Hydrogen is a well-known bulk impurity in rare-earth metals, and therefore the extent of the hydrogen coverage is likely to be due as much to the bulk content as to adsorption from the vacuum. From a comparison with published data we estimate the coverage of O and H on the as-prepared surface to be 2% and 7%, respectively. The hydrogen-induced peak is not due to intrinsic emission from hydrogen atoms, but rather represents a shift of the binding energy of the surface state upon adsorption of H_2 , which dissociates to leave H atoms in interstitial subsurface sites.⁴ The rare earths are thus one of the few groups of metals for which hydrogen has a signature in photoemission spectroscopy, clearly important in the investigation of possible dissociative adsorption of hydrogen-

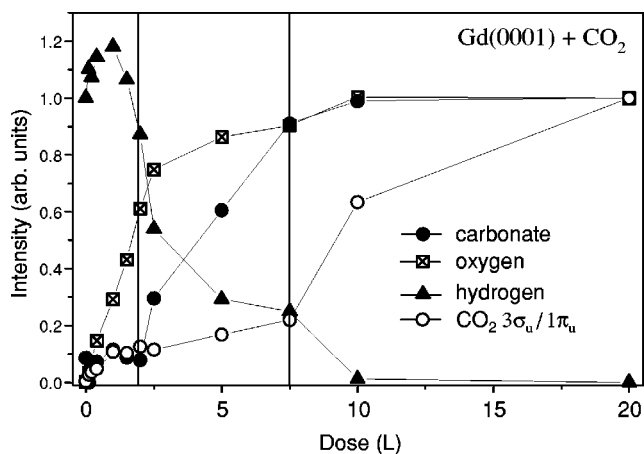
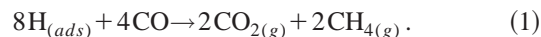


FIG. 2. Intensities of some of the photoemission features, as a function of exposure, for CO_2 on Gd(0001), derived from the data of Fig. 1. For clarity the intensities have been arbitrarily normalized.

containing molecules. At higher doses additional peaks appear—the molecular orbitals of CO_2 at binding energies > 8 eV, and a peak at 2.3 eV. This latter peak appears very similar to that at the same binding energy for CO adsorption on Gd(0001),^{6,14} where it was attributed to carbonate formation, and it seems reasonable to assign this feature to carbonate in this case also. The intensities of some of these peaks are plotted as a function of dose in Fig. 2. For the initial few doses of CO_2 the hydrogen peak can be seen to be increasing. Obviously this is not due to CO_2 adsorption, but rather represents an increase of the hydrogen coverage with time, due to adsorption from the UHV background. At data acquisition time, including the time to dose the sample, of ≈ 5 min/spectrum with a partial hydrogen pressure of 5×10^{-11} mbar, this is equivalent to a dose of 0.1 L over the first five spectra. Since at low coverages the sticking coefficient for hydrogen on Gd(0001) is close to unity,⁴ such a small dose from the background is capable of producing a significant increase in the hydrogen coverage. As the CO_2 dose increases the hydrogen peak begins to decrease, becoming unobservable at a total dose of 5 L. This indicates that a clean-up reaction is in progress, as has also been observed for CO on hydrogen predosed Gd(0001).⁶ In that case, since no additional peaks were observed to occur during the clean-up reaction, the products were entirely gaseous, with the reaction being of the form⁶



From the data of Fig. 1 it can be seen that while the hydrogen peak is decreasing, the oxygen peak is increasing, indicating that in this case the products of the reaction are not entirely gaseous, as oxygen is clearly being added to the surface. A possible scheme for the initial phase of CO_2 adsorption, i.e., the hydrogen clean-up reaction, is thus



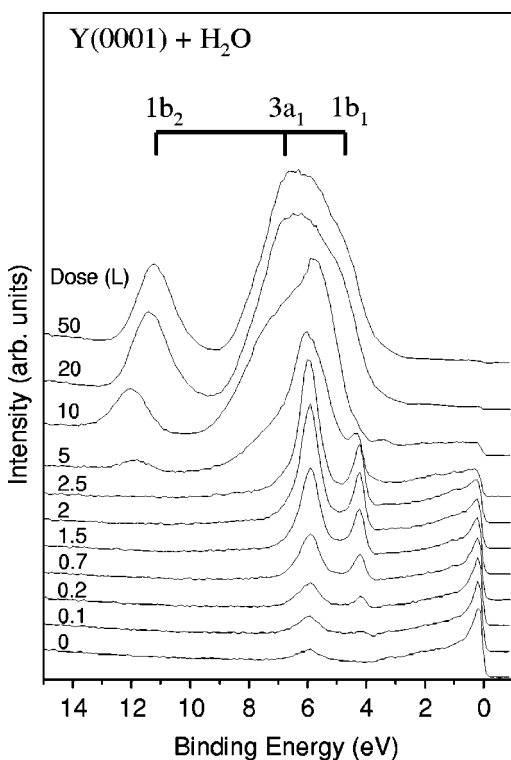


FIG. 3. Photoemission spectra ($h\nu=40$ eV) of Y(0001) with increasing exposure to H_2O . The assignments for the molecular orbitals of H_2O are also shown.

Before the hydrogen clean up has finished, carbonate formation begins. This suggests that on hydrogen-free areas of the surface, dissociative adsorption is occurring to give carbonate. Monolayer coverage can be approximately determined by observing the point at which the surface state disappears.⁴ This cannot be simply observed using the peak intensity, since the underlying bulk density of states also peaks at the Fermi level,¹⁷ albeit much less sharply. At a dose of 7.5 L the valence band shows the triangular form of the bulk density of states,¹⁷ with no indication of the sharp surface state, and so we assign this dose as resulting in monolayer coverage. At higher doses the molecular orbitals of CO_2 become apparent, while the intensities of the oxygen and carbonate peaks remain essentially unchanged. The oxygen peak becomes broadened, indicating the formation of some Gd_2O_3 ,¹¹ which is consistent with the shift to higher binding energy of the Gd $4f$ peak,¹¹ although this is somewhat obscured by the CO_2 $1\pi_g$ orbital.

The adsorption of CO_2 thus appears to proceed in three distinct phases: (1) hydrogen clean up, leaving adsorbed oxygen, (2) continued clean up, accompanied by dissociative adsorption of CO_2 giving carbonate, until monolayer coverage is reached, and (3) oxidation of Gd accompanied by molecular adsorption of CO_2 . In general, the data of Fig. 1 show very similar behavior to that of CO on Gd(0001), and in fact the spectrum for a CO_2 dose of 7.5 L in Fig. 1, i.e., monolayer coverage, is very similar to that of 7.4 L of CO on Gd(0001),¹⁴ which was taken using the same UHV system, with the exception that the O $2p$ peak is rather higher for the

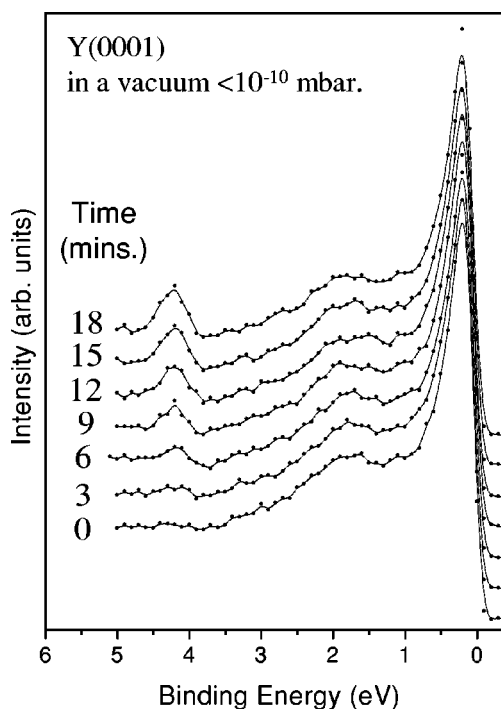


FIG. 4. Photoemission spectra ($h\nu=40$ eV) of as-deposited Y(0001), as a function of time, in a vacuum $<10^{-10}$ mbar, showing the growth of the hydrogen induced peak at a binding energy of 4 eV.

CO_2 data, as would be expected given the higher oxygen content of the adsorbing molecule.

B. H_2O on Y(0001)

Photoemission spectra of increasing doses of H_2O on Y(0001) are shown in Fig. 3. The as-prepared Y(0001) spectrum shows most of the same features as are seen on Gd(0001)—the surface state at the Fermi level, the bulk peak, in this case not so well resolved, at ~ 2 eV, and the adventitious oxygen peak at 6 eV, indicating an oxygen coverage of $\sim 2\%$. The hydrogen peak seen in the as-prepared spectrum of Gd(0001) in Fig. 1 is not observed in the as-prepared Y(0001) spectrum of Fig. 3. However, as can be seen from Fig. 4, a hydrogen peak was observed to grow with time. The initial absence of the hydrogen peak suggests that the bulk impurity hydrogen content of the yttrium source material is rather lower than that for the gadolinium, while the rapid growth of the hydrogen peak with time suggests that the sticking coefficient of hydrogen on Y(0001) is similar to that on Gd(0001). More explicit hydrogen dosing experiments would be needed to confirm this.

With initial H_2O dosing only an increase in the oxygen peak, accompanied by the growth of the hydrogen peak, is observed. As with Gd(0001), adsorption attenuates the surface state, allowing the estimation of monolayer coverage, which in this case occurs for a total dose of 2.5 L. At higher dosages the H_2O molecular orbitals become apparent. The intensities of some of the features in Fig. 3 are plotted as a function of coverage in Fig. 5. While some of the initial increase in the hydrogen peak intensity can be attributed to

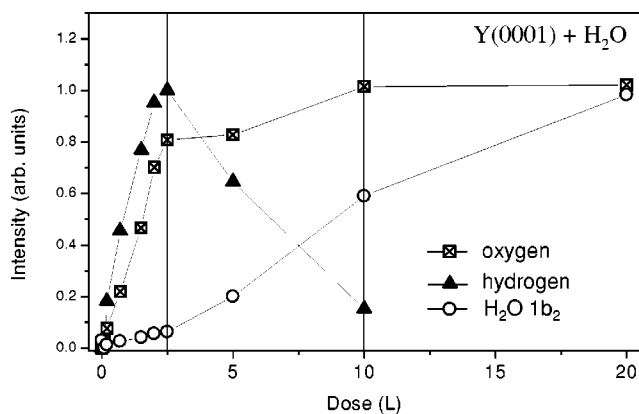


FIG. 5. Intensities of some of the photoemission features, as a function of exposure, for H_2O on $\text{Y}(0001)$, derived from the data of Fig. 3. For clarity the intensities have been arbitrarily normalized.

adsorption from the background, from these data it is clear that initial H_2O adsorption is entirely dissociative, until monolayer coverage is reached, after which molecular adsorption proceeds. From the continued suppression of the monolayer features with increasing exposure, including the Y Fermi level, it is clear that multilayers are being formed. Note that the binding energies of the H_2O $1b_2$ and $3a_1$ peaks change with increasing dosage. Determination of any binding energy shifts relative to the $1b_1$ peak, between initial molecular adsorption and the relatively thick (multilayer) film, is impeded by the presence of the O $2p$ peak from the dissociated monolayer, so from these data we cannot determine if the initial molecular layer is chemisorbed. Fig. 6 shows the Y $4p$ levels before and after H_2O adsorption. They show a clear shift to higher binding energy and significant broadening, consistent with the known behavior of Y $3d$ core levels upon oxidation to Y_2O_3 .²⁷ It thus appears that the

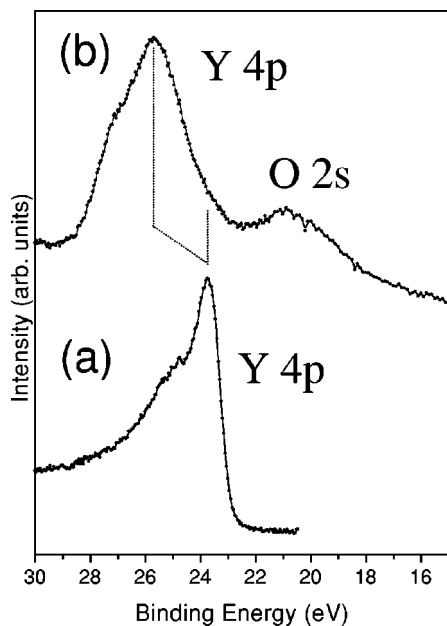


FIG. 6. Photoemission spectra ($h\nu=60$ eV) of the $4p$ region of (a) $\text{Y}(0001)$ and (b) $\text{Y}(0001)$ exposed to 50 L H_2O .

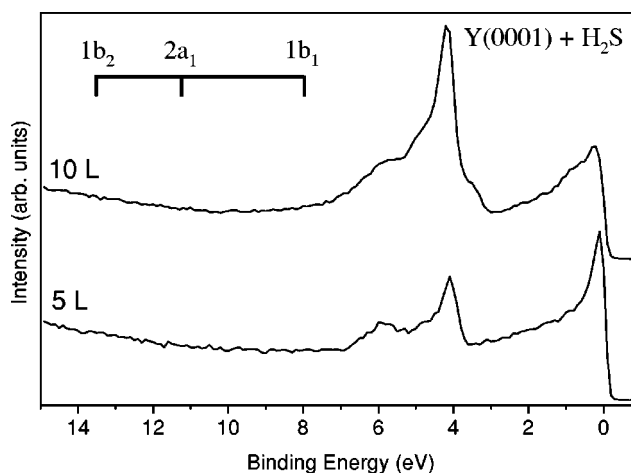


FIG. 7. Photoemission spectra ($h\nu=40$ eV) of $\text{Y}(0001)$ exposed to H_2S .

dissociative adsorption of H_2O is accompanied by oxidation of the $\text{Y}(0001)$ surface to Y_2O_3 .

C. H_2S and CH_4 on $\text{Y}(0001)$

Photoemission spectra from two doses of H_2S on $\text{Y}(0001)$ are shown in Fig. 7. Also shown are the expected binding energies of the H_2S molecular orbitals, taken from the gas phase spectrum of Rabalais,²⁶ aligned to the vacuum level, assuming a Y work function of 3.1 eV.²⁸ Since the timescale of the experiment was significantly shorter than that of the data of fig. 4, the hydrogen-induced peak seen in Fig. 7 can be largely attributed to the dissociation of H_2S . From the triangular line shape of the 10 L spectrum, we speculate that this exposure has produced a coverage close to monolayer. At this coverage additional shoulders to both the high and low binding-energy sides of the hydrogen peak can be seen. Atomic S has been seen to give rise to peaks in the binding-energy range 2.5–5.5 eV in ultraviolet photoemission spectroscopy (UPS) spectra of S on Pt,²⁹ W,³⁰ and Ru³¹ due to the S $3p$ level, and it seems reasonable to assume that this is also the case on $\text{Y}(0001)$. Therefore we assign the shoulders seen in fig. 5 as due to atomic sulfur $3p$ levels. In neither spectrum is there any indication of the H_2S molecular orbitals. These data suggest that, at least at submonolayer to-monolayer coverages, H_2S adsorption is entirely dissociative.

The S $2p$ spectrum of monolayer coverage is shown in Fig. 8. The binding energy of the S $2p_{3/2}$ peak can be seen to be ~ 162 eV, consistent with that for atomic sulfur on transition metals.²⁹ For S on the (close packed) Pt(111) surface, the S $2p$ data show two S $2p$ doublets, attributed to atomic sulfur in hollow and bridge sites, with a binding-energy difference of 0.94 eV. Although the data of Fig. 8 are not of particularly high quality, the photon energy used being at the high end of the usable range of the beamline,²¹ they show clear indication of two $2p$ doublets. To obtain an estimate of the relative binding energies, we employed a curve-fitting procedure, after subtracting a background as shown in Fig. 8. The background subtracted data were fit with two doublets,

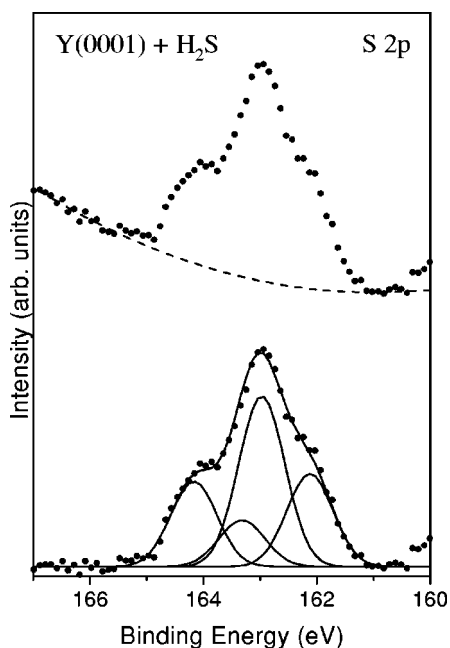


FIG. 8. S $2p$ photoemission spectrum ($h\nu=195$ eV) for Y(0001) + 10 L H_2S .

each constrained to have a spin-orbit splitting of 1.2 eV (Ref. 30) and a branching ratio of 2:1. As an approximation, given the rather poor quality of the data, in terms of resolution and statistics, and the uncertainties introduced by the proximity of the Y $3d$ peak (the rising background to lower binding energy),³² the line shape used was a Gaussian, with full width at half maximum of 0.8 eV. The binding-energy separation of the two doublets determined from the fitting procedure was found to be 0.8 eV, consistent with the results for S on Pt(111),²⁹ especially when the quality of the data of Fig. 8 is taken into account. This suggests that adsorption in both hollow and bridge sites occurs for S on Y(0001).

Aside from the growth of the hydrogen peak due to background exposure as shown in Fig. 4, no additional features were observed when dosing CH_4 on Y(0001), even at exposures >100 L. If we assume that a coverage of 1% would be visible in the photoemission spectra, this implies that the sticking coefficient for CH_4 on Y(0001) at room temperature is $<10^{-4}$, clearly orders of magnitude lower than for all the other adsorbates studied on rare-earth (0001) surfaces.

D. Comparison with single-crystal data

The spectrum of a Y(0001) single crystal³³ and that of the as-prepared Y(0001) film on W(110) are compared in Fig. 9. While the spectra are very different it should be noted that all the features present on the Y(0001)/W(110) film are also evident on the single crystal: the surface state close to the Fermi level, the bulk state at 2 eV, and the adventitious oxygen peak at 6 eV. Similar features have been observed for many other rare-earth metal (0001) surfaces.³⁴ The 7 eV peak on the single crystal, initially assigned to a many-body state in Ref. 33 has been shown to be due, in fact, to chlorine impurities.³⁵ This leaves the significant differences between the two spectra as the peaks at 9.6 eV and 3 eV. The prop-

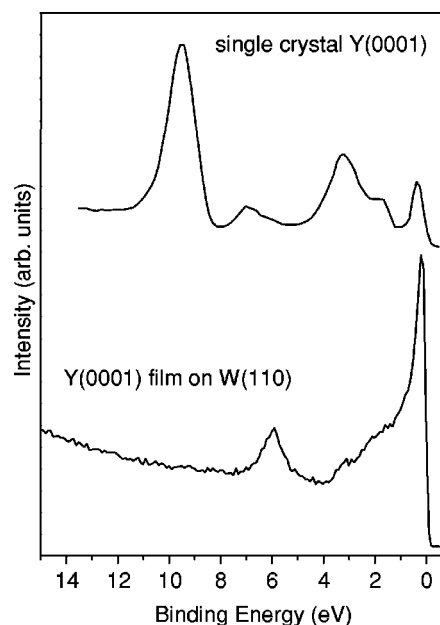


FIG. 9. Photoemission spectrum of a Y(0001) film on W(110) compared to that of a nominally clean surface of single crystal Y(0001) from Ref. 33. The photon energy (40 eV) and experimental geometry were the same for both spectra.

erties of these peaks are discussed in detail in Ref. 34, but they have always been observed together. While the suggestion that they may result from many-body surface-related states has been put forward,^{33,34} there remains no explanation of how these peaks could be intrinsic features. The presence of these effectively unexplained peaks in the single-crystal data, and the resulting differences with the thin-film (0001) data, has led to the single-crystal data being either ignored or summarily dismissed. While it seems clear to the community, including the present authors, that the thin-film data are far more representative of the intrinsic rare-earth metal surface electronic structure, it is also true, and rather puzzling, that no explanation for the possible extrinsic source of the unexplained features has been presented.

With the addition of the H_2O , CO_2 , and H_2S data from this work, and the observations regarding CH_4 , there is now a reasonable body of data regarding adsorbates, at both high and low coverages, on rare-earth (0001) surfaces. These data are summarized in Fig. 10. Spectra from C_2H_4 and C_2H_2 on single crystal Gd(0001) are also included in Fig. 10.³⁶ This substrate was prepared in such a way as to reproduce neither the other literature data for single crystal Gd(0001)^{37,38} nor the thin film data, but has been included for completeness. The range of adsorbates in Fig. 10 includes all the common UHV residual gasses, i.e., H_2 , CH_4 , H_2O , CO , and CO_2 , and even the consequences of an air leak (N_2 and O_2). The adsorbate data also show peaks due to atomic species of several impurities that might be expected in the bulk material, i.e. H, C, O, and S. Note that for none of these spectra is a peak at either 9.6 eV or 3 eV observed. This suggests that, whatever the cause of the unexplained peaks in the single-crystal data, it is not merely a case of common impurities or adventitious adsorbates.

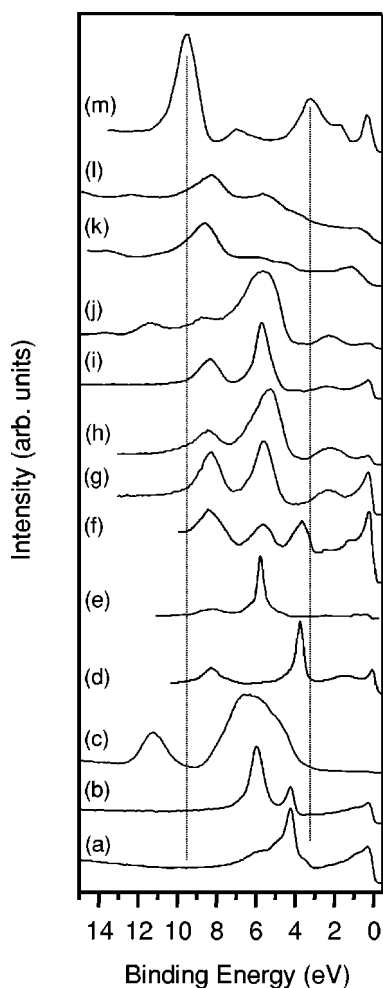


FIG. 10. Photoemission spectra of rare-earth (0001) surfaces with different adsorbates. (a) Y + 10 L H₂S, (b) Y + monolayer H₂O, (c) Y + 50 L H₂O, (d) Gd + monolayer H₂ (Ref. 4), (e) Gd + monolayer O₂ (Ref. 11), (f) Gd + 0.45 monolayer N₂ (Ref. 13), (g) Gd + monolayer CO (Ref. 14), (h) Gd + 7.4 L CO (Ref. 14), (i) Gd + monolayer CO₂, (j) Gd + 20 L CO₂, (k) Gd + C₂H₂ (Ref. 36), (l) Gd + C₂H₄ (Ref. 36). Also shown, (m), is a spectrum of nominally clean single crystal Y(0001) (Ref. 33).

IV. CONCLUSIONS

From a comparison with the range of adsorbates on rare-earth metals now available in the literature, it appears that the unexplained peaks in the single-crystal rare-earth photo-

emission data cannot be explained simply in terms of common impurities or adventitious adsorbates. While it remains clear that the thin-film data are far more representative of the intrinsic rare-earth metal (0001) surfaces, the lack of an apparent simple explanation in terms of contamination suggests that these peaks are worthy of further study.

For the molecules which were found to adsorb at room temperature, CO₂, H₂O, and H₂S, initial adsorption appears to be entirely dissociative, accompanied by the apparent formation of carbonate and oxide species for CO₂ and H₂O adsorption, respectively. The results imply that adventitious hydrogen on Gd(0001) is removed by CO₂ in a clean-up reaction, which leaves adsorbed oxygen on the surface. This is analogous behavior to that observed for CO on hydrogen predosed Gd(0001),⁶ but, since the products are not entirely gaseous, clearly proceeds via a different mechanism that proposed by Getzlaff *et al.*⁶ for CO/H coadsorption. The data for H₂S on Y(0001) suggest that atomic sulfur remains on the surface, adsorbing in both hollow and bridge sites, although due to the limited dataset these conclusions should be regarded as preliminary.

Unlike all the other molecules studied on well-characterized rare-earth metal surfaces to date, CH₄ was found not to adsorb on Y(0001) at room temperature. With the exception of H₂, whose affinity for rare-earth metal interstitial sites is well known, CH₄ is the only fully saturated molecule among the molecules studied to date, containing no π bonds or lone pairs with which to interact with a metallic surface. Therefore the lack of interaction with Y(0001) is not surprising.

The apparent ability of rare-earth surfaces to dissociate almost all adsorbates is in contrast to the behavior seen for adsorbates on other transition-metal surfaces, where chemisorption of intact molecules at room temperature is far from uncommon. This cannot be related to mixed-valence behavior since both Y and Gd have a stable trivalent configuration. This suggests the possibility that the ability of rare earths to catalytically oxidize W and Ta surfaces¹⁸⁻²⁰ may not be due to a redox reaction, but more simply due to the higher reactivity of the atomic oxygen produced by dissociative adsorption of O₂ on the rare-earth surface.

ACKNOWLEDGMENTS

We would like to thank Andy Robinson, for assistance at DL, and the UK EPSRC and Agilent Technologies for funding.

*Electronic address: rob.blyth@unile.it

¹S.D. Barrett and S.S. Dhesi, *The Structure of Rare-Earth Metal Surfaces* (Imperial College Press, London, 2001).

²S.C. Kim, S.N. Kwon, M.-W. Choi, C.N. Whang, K. Jeong, S.H. Lee, J.-G. Le, and S. Kim, *Appl. Phys. Lett.* **79**, 3726 (2001).

³N. Koch, E. Zojer, A. Rajagopal, J. Ghijsen, R.L. Johnson, G. Leising, and J.-J. Pireaux, *Adv. Funct. Mater.* **11**, 58 (2001).

⁴D. Li, Z. Zhang, P.A. Dowben, and M. Onellion, *Phys. Rev. B* **48**, 5612 (1993).

⁵M. Getzlaff, M. Bode, and R. Wiesendanger, *Surf. Sci.* **410**, 189 (1998).

⁶M. Getzlaff, M. Bode, R. Pascal, and R. Wiesendanger, *Phys. Rev. B* **59**, 8195 (1999).

⁷M. Getzlaff, M. Bode, R. Pascal, and R. Wiesendanger, *Appl. Surf. Sci.* **142**, 63 (1999).

⁸E. Vescovo, O. Rader, T. Kachel, U. Alkemper, and C. Carbone, *Phys. Rev. B* **47**, 13 899 (1993).

⁹J. Zhang, P.A. Dowben, D. Li, and M. Onellion, *Surf. Sci.* **329**, 177 (1995).

¹⁰M. Getzlaff, J. Paul, J. Bansmann, C. Ostertag, G.H. Fecher, and G. Schönense, *Surf. Sci.* **352**, 123 (1996).

¹¹C. Schüssler-Langeheine, H. Ott, Z. Hu, C. Mazumdar, A.Y. Grig-

- oriev, G. Kaindl, and E. Weschke, *Phys. Rev. B* **60**, 3449 (1999).
- ¹²C. Schüssler-Langeheine, H. Ott, A.Y. Grigoriev, A. Müller, R. Meier, Z. Hu, C. Mazumdar, G. Kaindl, and E. Weschke, *Phys. Rev. B* **65**, 214410 (2002).
- ¹³C. Waldfried, D.N. McIlroy, D. Li, J. Pearson, S.D. Bader, and P.A. Dowben, *Surf. Sci.* **341**, L1072 (1995).
- ¹⁴C. Searle, R.I.R. Blyth, R.G. White, N.P. Tucker, M.H. Lee, and S.D. Barrett, *J. Synchrotron Radiat.* **2**, 312 (1995).
- ¹⁵J.K. Lang, Y. Baer, and P.A. Cox, *J. Phys. F: Met. Phys.* **11**, 121 (1981).
- ¹⁶P. Blaha, K. Schwartz, and P.H. Dederichs, *Phys. Rev. B* **38**, 9368 (1988).
- ¹⁷R. Wu, C. Li, A.J. Freeman, and C.L. Fu, *Phys. Rev. B* **44**, 9400 (1991).
- ¹⁸E.E. Latta and M. Ronay, *Phys. Rev. Lett.* **53**, 948 (1984).
- ¹⁹M. Ronay and E.E. Latta, *Phys. Rev. B* **32**, 5375 (1985).
- ²⁰C. Gu, C.G. Olsen, and D.W. Lynch, *Phys. Rev. B* **48**, 12 178 (1993).
- ²¹V.R. Dhanak, A.W. Robinson, G. van der Laan, and G. Thornton, *Rev. Sci. Instrum.* **63**, 1342 (1992).
- ²²N.P. Tucker, R.I.R. Blyth, R.G. White, M.H. Lee, C. Searle, and S.D. Barrett, *J. Phys.: Condens. Matter* **10**, 6677 (1998).
- ²³E. Weschke and G. Kaindl, *J. Electron Spectrosc. Relat. Phenom.* **75**, 233 (1995).
- ²⁴G. Kaindl, A. Höhr, E. Weschke, S. Vandre, C. Schüssler-Langeheine, and C. Laubschat, *Phys. Rev. B* **51**, 7920 (1995).
- ²⁵B. Kim, A.B. Andrews, J.L. Erskine, K.J. Kim, and B.N. Harmon, *Phys. Rev. Lett.* **68**, 1931 (1992).
- ²⁶J.W. Rabalais, *Principles of UPS* (Wiley, New York, 1977).
- ²⁷R.P. Vasquez, M.C. Foote, and B.D. Hunt, *J. Appl. Phys.* **66**, 4866 (1989).
- ²⁸K.F. Wojciechowski, *Vacuum* **48**, 891 (1997).
- ²⁹J.A. Rodriguez, M. Kuhn, and J. Hrbek, *Chem. Phys. Lett.* **251**, 13 (1996).
- ³⁰D.R. Mullins, P.F. Lyman, and S.H. Overbury, *Surf. Sci.* **277**, 64 (1992).
- ³¹J. Hrbek, M. Kuhn, and J.A. Rodriguez, *Surf. Sci.* **356**, L423 (1996).
- ³²R.P. Vasquez, *J. Electron Spectrosc. Relat. Phenom.* **50**, 167 (1990).
- ³³S.D. Barrett and R.G. Jordan, *Z. Phys. B: Condens. Matter* **66**, 375 (1987).
- ³⁴S.D. Barrett, *Surf. Sci. Rep.* **14**, 271 (1992).
- ³⁵R.G. White, Ph.D. thesis, University of Liverpool, 1996 (unpublished).
- ³⁶R.J. Simonson, J.R. Wang, and S.T. Ceyer, *J. Phys. Chem.* **91**, 5681 (1987).
- ³⁷F.J. Himpsel and B. Riehl, *Phys. Rev. B* **28**, 574 (1983).
- ³⁸R.G. Jordan, *Phys. Scr., T* **13**, 22 (1986).